ACS OMEGA

Open Access

http://pubs.acs.org/journal/acsodf

Article

Cytotoxic Activity of Phytoconstituents Isolated from *Monotheca buxifolia* against Hepatocellular Carcinoma Cell Line HepG2: In Vitro and Molecular Docking Studies

Published as part of the ACS Omega virtual special issue "Phytochemistry".

Said Hassan, Bashir Ahmad,* Muhammad Waseem Khan, Zafar Abbass Shah, Amin Ullah, Sana Ullah, Dilfaraz Khan, Muhammad Rizwan, Ajaz Ahmad, Qurban Ali,* Prashant Kaushik, and Semih Yilmaz

Cite This: *ACS Omega* 2023, 8, 33572−33579

Read Online

ACCESS | Metrics & More | Article Recommendations

ABSTRACT: Natural products and conventional chemotherapeutic drugs are believed to enhance anticancer treatment efficacy while lowering toxicity. The current study investigates the cytotoxic and apoptogenic effects of *Monotheca buxifolia* bioactive compounds on HepG2 cell lines. MTT assay was used to assess the effect on the viability of HepG2 cells. Morphological changes were investigated. Annexin-V-FITC/PI was used to demonstrate apoptotic activity. A molecular dynamics simulation study was carried out to investigate the compound binding pattern in the active site of the PPRAδ protein. MTT and annexin V-FITC/PI assays revealed that the isolated compounds lauric acid, oleanolic acid, and bis(2-ethylhexyl) phthalate inhibited the growth of hepatocellular cancer cells. The IC_{50} value for lauric acid was 56.46 ± 1.20 μg/mL, 31.94 ± 1.03 μg/mL for oleanolic acid, and 83.80 ± 2.18 μg/mL for bis(2-ethylhexyl) phthalate. Apoptosis was observed in 29.5, 52.1 and 22.4% of HepG2 cells treated with lauric acid, oleanolic acid, and bis(2-ethylhexyl) phthalate, respectively, after 24 h of treatment. Morphological assays and Hoechst staining microscopy revealed that the treatment caused morphological changes in the cell membrane and nuclear condensation. The high fluctuation indicates that various interactions were highly potent and widely adopted, and vice versa. Oleanolic acid displayed high residue fluctuation, remaining stable in the active site of the PPRAδ protein and involved in various interactions while remaining locally fluctuating in the binding sites of the other two compounds. These findings concluded that lauric acid, oleanolic acid, and bis(2-ethylhexyl) phthalate have a significant apoptogenic effect against HepG2 cells in inducing apoptosis. Our findings suggest that these bioactive compounds could be used as adjuvant therapies.

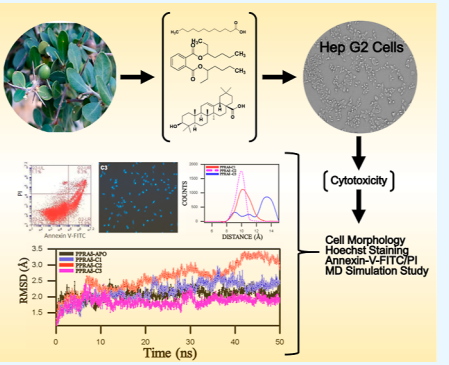

1. INTRODUCTION

Natural resources, such as plants, microbes, vertebrates, and invertebrates, are valuable sources of bioactive compounds. Natural products are compounds or materials that could be acquired from living organisms, including animals, plant life, insects, venom, and microorganisms.[1] Biologically active ingredients with therapeutic, commercial, and toxic properties have been explored all over the world and have many secondary metabolite ingredients.[2] It is estimated that about 50% of drugs have been acquired from herbal products.[3]

Cancer cells involve abrupt cell divisions that proliferate in normal cells of the body, and in the end, cancerous cells damage the attached tissues. These damaged tissues result in malfunctioning organs and can be the cause of death.[4,5] Globally, after heart disease, cancer is the leading cause of death, with an estimated ten million cases of various types of malignancies reported each year.[6] In the beginning, advanced of the insecticides' ability of the natural products, the lethal dose toxicity activity is now the easiest, in a short time, a robust and globally acceptable procedure for evaluating anticancer capacity.[7] Ethno-medicinal uses of natural products derived from plants are the major sources for the discovery of potential anticancer agents.[8] Natural products are primary sources of effective anticancer drugs with novel structures and unique mechanisms of action for the treatment of various forms of cancer.[9] Various plant-derived natural products such as saponins, alkaloids, flavonoids, terpenes, and polysaccharides have been used against hepatocellular carcinoma (HCC).[10]

Received: May 26, 2023
Accepted: August 23, 2023
Published: September 2, 2023

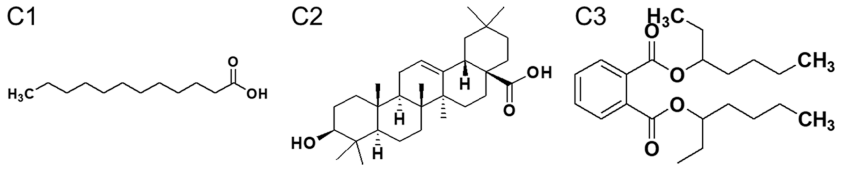

Figure 1. Chemicals structures of C1 (lauric acid), C2 (oleanolic acid), and C3 (bis(2-ethylhexyl) phthalate) isolated from *M. buxifolia*.

HCC affects all sectors of the world population. It is the fifth universal cancer among other cancers and has the second-highest mortality rate among all cancers.[11] Liver cancer is a growing global health challenge, with an estimated annual incidence of >1 million cases worldwide by 2025. HCC accounts for approximately 90% of the cases of liver cancer and is associated with high morbidity and mortality.[12]

Monotheca buxifolia species are found in hilly areas of Pakistan and have therapeutic uses such as antiseptic, for relieving gastrointestinal disorders, analgesic, anti-inflammatory, antipyretic, and for wound healings.[13] These plants are abundant in Dir Lower, Attock, Xhob Kala Chitta, and Chitral.[14] In this study, cytotoxic and apoptotic activities and computational studies of lauric acid, oleanolic acid, and bis (2-ethylhexyl) phthalate bioactive compounds from *M. buxifolia* were carried out, which might lead to the potential management of hepatocellular carcinoma.

2. MATERIAL AND METHODOLOGY

2.1. Plant Collection. Aerial parts of *M. buxifolia* (15 kg), a wild-type fruiting plant grown in arid and semiarid climate conditions, were collected from District Dir Lower, Khyber Pakhtunkhwa-Pakistan with voucher ID MBDDL20200103 and voucher specimens were deposited in a public herbarium of District Dir Lower. Dr. Jehandar Shah, the Taxonomist, Ex-Vice Chancellor, Shaheed Benazir University Shiringal, Pakistan, authenticated the plant samples. It has been confirmed that the experimental samples of plants, including the collection of plant material, complied with relevant institutional, national, and international guidelines and legislation with appropriate permissions from District authorities of Dir Lower Khyber Pakhtunkhwa-Pakistan for the collection of plant specimens. The plants were thoroughly cleaned with tap water and rinsed with distilled water. Plant materials were dried under shade at room temperature. Next, the plant was chopped to make a powder.[15] It has been confirmed that the experimental research and field studies on plants, including the collection of plant material, complied with relevant institutional, national, and international guidelines and legislation with appropriate permission from the Research Institute for the collection of plant specimens.

2.2. Extraction and Isolation. Dried aerial parts of the plants were chopped, cut into pieces, and ground into a fine powder by using an electric grinder. The powder materials of *M. buxifolia* (15 kg each) were soaked three times in methanol for 15 days with random shaking at room temperature; after completion of the immersing, the methanolic soluble portion was filtered. The filtrate was concentrated using a rotary evaporator at 40 °C, and 500 g of a blackish methanolic extract was obtained from *M. buxifolia*. The MeOH extract was suspended in water and successively partitioned with hexane, dichloromethane, and ethyl acetate (EtOAc).[16] The EtOAc fraction (90 g) was subjected to column chromatography on silica gel (Merck silica gel 60 (0.063−0.200 mm), 5 × 60 cm). As a solvent system, the column was first eluted with hexane-EtOAc (100:0 → 0:100). A total of 30 fractions, SH-1 to SH-30, were obtained based on thin-layer chromatography (TLC) profiles. Lauric acid (15 mg), oleanolic acid (18 mg), and bis (2-ethylhexyl) phthalate (12 mg) were isolated with the help of flash chromatography from the subsequent fractions.[17] The purity of the compound was confirmed by TLC and further characterized by NMR (Figure 1.

2.3. Cytotoxic Assay against HepG2 Cells. ATCC, Manassas, VA, USA, provided the HepG2 cells. The MTT procedure was used to assess cell death.[18] Briefly, 96-well plates were used to seed 5×10^4 cells/mL. Cells were seeded for 24 h; after 24 h, cells were treated with concentrations of 100 and 75 μg/mL of lauric acid, oleanolic acid, and bis(2-ethylhexyl) phthalate and incubated for 48 h. Dimethyl sulfoxide (DMSO, 0.5%) was treated as the negative control. After removal of the medium, 1 mg/mL MTT reagents (Thermo Fisher USA catalog number: M6494) were added to each well. The incubation of plates was carried out for 2 h at 37 °C in a 5% CO_2 atmosphere. MTT reagents were removed after incubation, and formazan violet was dissolved in 100 μL of DMSO. Sample absorbance was calculated by using microplate readers at a wavelength of 570 nm. The readings obtained from the samples were compared with those of the control, whose viability is 100%. The IC_{50} (μg/mL) values of the cancerous cells were calculated. The experiments were performed in triplicate.[19]

2.4. Cell Apoptosis Study. Cell Morphology. Morphological observation of cells treated with lauric acid, oleanolic acid, and bis(2-ethylhexyl) phthalate was done to determine the changes induced by lauric acid, oleanolic acid, and bis(2-ethylhexyl) phthalate. All cells were exposed to increasing concentrations (100 μg/mL) of lauric acid, oleanolic acid, and bis(2-ethylhexyl) phthalate for 24 h, and cell images were taken using an inverted phase-contrast microscope (OLYMPUS CKX 41) at 10× magnification.[20]

2.5. Hoechst 33258 Staining Assay. Hoechst 33258 staining assay was carried out to evaluate cell apoptosis as previously reported[21] with minor modifications. HepG2 cells were seeded into 6-well plates overnight and then treated with 100 μg/mL lauric acid, oleanolic acid, and bis(2-ethylhexyl) phthalate for 24 h. The wells were washed three times with PBS and fixed with 4% paraformaldehyde (500 μL) for 30 min. The cells were washed three times with PBS, followed by staining with Hoechst 33258 (500 μL, 5 μg/mL) for 10 min at 37 °C in the dark. After being washed three times with PBS, the cells were visualized with a fluorescence microscope (IX71; Olympus, Japan).

2.6. Annexin V-FITC/PI Assay. Compounds isolated from *M. buxifolia* were assessed for an apoptotic study against HepG2 cells. The apoptosis of the isolated compounds was calculated by flow cytometry. 2×10^5 cells were cultured in 75 cm^2 flasks with appended culture medium for 24 h. HepG2 cells were treated with 100 μg/mL lauric acid, oleanolic acid, and bis(2-ethylhexyl) phthalate for 24 h. A hydroalcoholic

https://doi.org/10.1021/acsomega.3c03705
ACS Omega 2023, 8, 33572−33579

solution was used as the negative control. Annexin V/PI assay was performed according to the PI/FITC apoptosis kit protocol. HepG2 cells were harvested, washed with a PBS buffer solution, and kept in a sterilized tube. The cell pellets were suspended in 100 μL of binding buffer. The cell suspensions were shifted to a microtube, to which 5 μL of Annexin-V/FITC conjugates and 10 μL of propidium-iodide (PI) were added. The incubation of cells was carried out for 15 min in the dark at room temperature. Flow cytometry was used to determine the fluorescence of the cells.[22] Ten thousand cells were quantified by a flow cytometer (BD). BD Bioscience-C6 software was used to analyze the data. The experiment was performed in triplicate.

2.7. Molecular Dynamics Simulation Study. To illustrate the binding mode of these selected compounds in the active pocket of peroxisome proliferator-activated receptors (PPAR), a molecular docking (MD) study was conducted using the MOE-Dock package.[23,24] The crystal structure of PPRAδ (PDB ID 1i7i)[25] was retrieved from the protein data bank. Before MD, the 3D protonation and energy minimization (EM) of the crystal structure were analyzed by using the default parameters of the MOE energy minimization algorithm (gradient: 0.05, Force Field: Amber99).[26] All of the selected compounds in the current study were downloaded from PubChem using PubChem ID 3893 for lauric acid, 10494 for oleanolic acid, and 8343 for bis(2-ethylhexyl) phthalate, indicated by the names lauric acid, oleanolic acid, and bis(2-ethylhexyl) phthalate thoroughly in the bioinformatics section. The EM for all compounds was carried out up to a 0.05 gradient using the MMFF94s force field implemented in the MOE. Finally, all selected compounds were docked into the active site of the protein utilizing the Triangular Matching docking method (default), and 100 different conformations for each compound were generated. The scores from the GBVI/WSA binding free energy (BFE) calculation ranked the predicted ligand−protein complexes. The GBVI/WSA is a scoring function that estimates the BFE of a given pose. For all scoring purposes, lower scores indicate a more favorable mode of interaction. The unit for scoring purposes is kcal/mol. The next top conformation of each compound was selected based on the docking score for further analysis. The predicted ligand−protein complexes were analyzed for molecular interactions in PyMol. More recently, the top conformer was further validated by a molecular dynamics (MD) simulation study to explore the dynamic behaviors of the selected compounds in the active cavity. A total of four systems were prepared for the MD simulation study; PPARδ-APO, PPARδ-C1, PPARδ-C2, and PPARδ-C3. The AMBER v14 tool was used to perform MD simulations; the topology of each compound was generated using the Antechamber module of AMBER. A 1.5 nm cubic box was solvated using the transferable intermolecular potential with 3 points (TIP3P) water model.[27,28] Sodium and chloride ions were added to the cubic box by the LEaP program to neutralize the overall system. These ions had the maximum electrostatic potential to replace the water molecules. The energy was minimized for 6000 cycles using the steepest descent and conjugate gradient minimization for 3000 cycles.[29] Equilibration was performed with moles (N), volume (V), and energy (E) (NVT) ensemble at 300 K, followed by NPT (amount of substance [N], pressure [P], and temperature [T]) for 300 K at a pressure of 1 bar for 2000 ps for each. The Berendsen thermostat method was applied for temperature,[30] while pressure was maintained constant, and the bond length was rectified with the linear constraint solver algorithm.

2.8. Statistical Analysis. The statistical analysis was done by the first author (Said Hassan) by applying Student's t-test using GraphPad Prism. The results are presented as mean ± SEM (standard error of the mean) of triplicates done for the same experiment or an average of three independent experiments (n = 3).

3. RESULTS AND DISCUSSION

Lauric acid, oleanolic acid, and bis(2-ethylhexyl) phthalate were isolated by column chromatography from the aerial parts of the *M. buxifolia* methanolic extract. NMR confirmed the purity and identification. The isolated compounds were evaluated for cytotoxic effects against the HepG2 cell line and their molecular docking.

3.1. Cytotoxic Assay of the Isolated Compounds against HepG2 Cells. The effect of lauric acid, oleanolic acid, and bis(2-ethylhexyl) phthalate on the viability of hepatocellular carcinoma cells was assessed by the MTT assay. The (%)-inhibition results from cell mortality after incubating the extracts for 48 h are shown in Figure 2; a concentration of 100

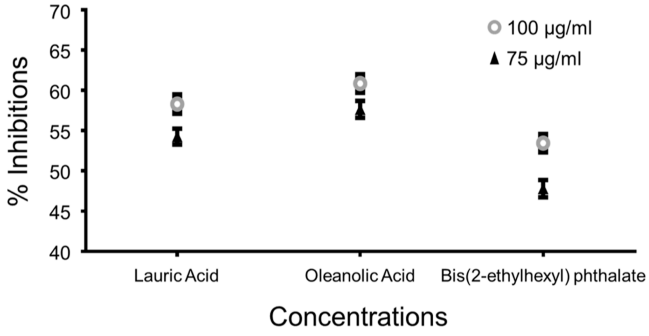

Figure 2. HepG2 cytotoxicity of lauric acid, oleanolic acid, and bis(2-ethylhexyl) phthalate (data are reported as the mean ± S.E.M).

μg/mL lauric acid shows 58.32 ± 1.09%, oleanolic acid shows 60.87 ± 1.05% and bis(2-ethylhexyl) phthalate shows 53.46 ± 1.03% cytotoxic potency against HepG2 cells while at concentration of 75 μg/mL lauric acid shows 54.27 ± 0.98%, oleanolic acid shows 57.65 ± 1.06% and bis(2-ethylhexyl) phthalate shows 47.81 ± 1.08% inhibition against HepG2 cells. The IC_{50} values are 56.46 ± 1.20 μg/mL for lauric acid, 31.94 ± 1.03 μg/mL for oleanolic acid, and 83.80 ± 2.18 μg/mL for bis(2-ethylhexyl) phthalate (Table 1). The following results

Table 1. IC_{50} Values of Lauric Acid, Oleanolic Acid, and Bis(2-ethylhexyl) Phthalate against HepG2 Cells

compounds	IC_{50} μg/mL
lauric acid (C1)	56.46 ± 1.20
oleanolic acid (C2)	31.94 ± 1.03
bis(2-ethylhexyl) phthalate (C3)	83.80 ± 2.18

further demonstrate that the cell lines were more sensitive to oleanolic acid and other compounds. It can be seen from the above study that all compounds have cytotoxic effects. Thus, these compounds could be used as a source for new lead structures in drug design to combat cancer.[31]

The active constituents, namely, flavonoids and terpenoids, may be responsible for reducing cancer risk factors.[32] The

https://doi.org/10.1021/acsomega.3c03705
ACS Omega 2023, 8, 33572−33579

anticancer effect against liver cancer on HepG2 cell lines showed that all three compounds possess an antiproliferative effect.

3.2. Cell Apoptosis Study. *3.2.1. Morphological Changes.* Morphological alteration of HepG2 cells after exposure to lauric acid (shown in Figure 3C1), oleanolic

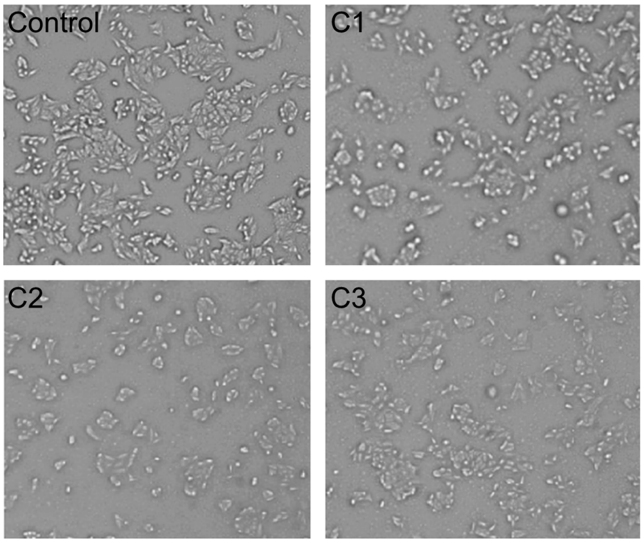

Figure 3. Morphological changes in HepG2 cells following the exposure to C1 (lauric acid), C2 (oleanolic acid), and C3 (bis(2-ethylhexyl) phthalate) after 24 h treatment. Images were taken using an inverted phase-contrast microscope at 10× magnification.

acid (shown in Figure 3C2), and bis(2-ethylhexyl) phthalate (shown in Figure 3C3) was observed under a phase-contrast microscope. The cells indicated the most prominent effects after exposure to lauric acid, oleanolic acid, and bis(2-ethylhexyl) phthalate. Changes in morphology were observed in treated cells. Exposure of the cells to 100 μg/mL lauric acid, oleanolic acid, and bis(2-ethylhexyl) phthalate for 24 h reduced the morphology of the cells and cell adhesion capacity in comparison to the control shown in Figure 3 control. Most of the cells lost their typical morphology and appeared smaller, shrunken, and rounded.

3.2.2. Hoechst 33258 Staining Assay. Staining cells with Hoechst 33258 is an ideal assay for distinguishing apoptotic cells from healthy or necrotic cells[33] because cells that have died by apoptosis will generally display condensed DNA and fragmented nuclei,[34,35] whereas healthy and necrotic cells do not. However, healthy cells undergoing mitosis may also have condensed DNA, and some cells can still die by apoptosis without nuclear fragmentation.[36] As shown in Figure 4, cells of the control group (Figure 4 control) had normal nuclear morphology under a fluorescent microscope after Hoechst 33258 staining, indicating that the chromatin was evenly distributed in the nucleus. The test group was marked with nuclear fragmentation, condensation of chromatin, and the morphological characteristics of apoptosis, which include emitting brighter fluorescence, after treatment with 100 μg/mL lauric acid (Figure 4C1), oleanolic acid (Figure 4C2) and bis(2-ethylhexyl) phthalate (Figure 4C3) for 24 h. These results indicated that lauric acid, oleanolic acid, and bis(2-ethylhexyl) phthalate can induce apoptosis in HepG2 cells.

3.2.3. Annexin V-FITC/PI Assay. Annexin V-FITC and PI staining assays are ways to detect the apoptotic level of cells.

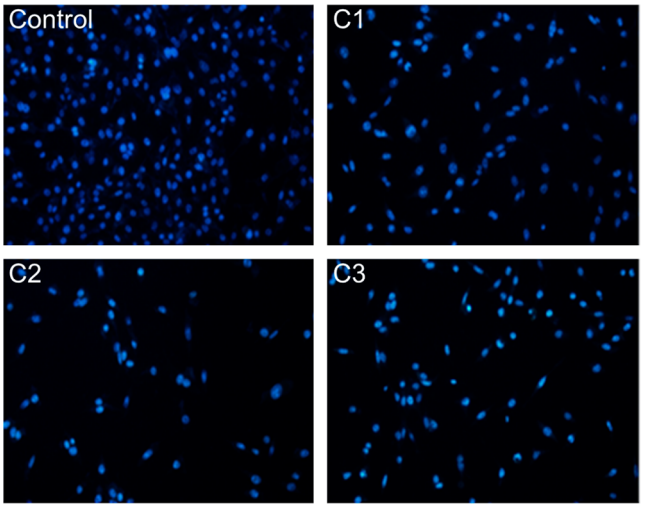

Figure 4. HepG2 cells treated with 100 μg/mL C1 (Lauric acid), C2 (oleanolic acid), and C3 (bis(2-ethylhexyl) phthalate) for 24 h were stained with nuclear stain (Hoechst 33258) and observed under fluorescent microscope 10× magnification.

Cells were exposed to no treatment (Figure 5 control) and to concentrations of 100 μg/mL lauric acid (Figure 5C1),

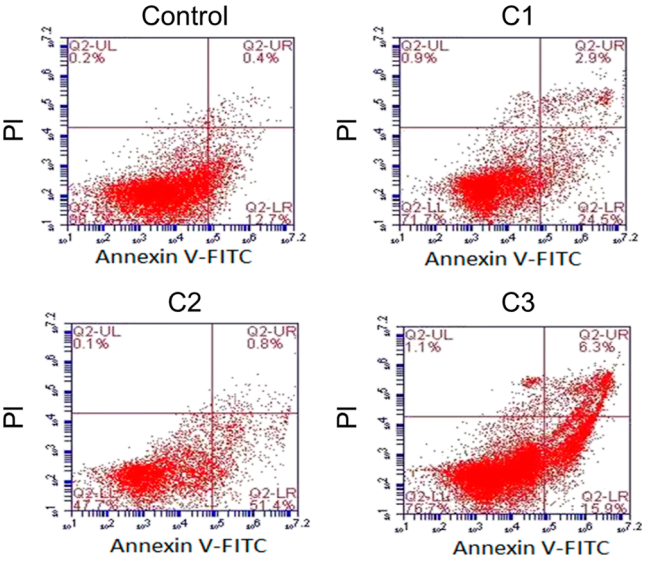

Figure 5. Annexin V and PI staining. C1 (lauric acid), C2 (oleanolic acid), and C3 (bis(2-ethylhexyl) phthalate).

oleanolic acid (Figure 5C2), and bis(2-ethylhexyl) phthalate (Figure 5C3). After 24 h, the percentage of apoptotic HepG2 cells treated with lauric acid was 24.5%, oleanolic acid was 51.4%, and bis(2-ethylhexyl) phthalate was 15.9%. A higher percentage of apoptotic cells was observed in wells treated with oleanolic acid than those treated with lauric acid and bis(2-ethylhexyl) phthalate. This result indicates that oleanolic acid has highly cytotoxic properties. Previously, oleanolic acid was tested to induce apoptosis in various cell lines.[37−39] The pharmaceutical industry can derive a bioactive compound responsible for the cytotoxic effect of bioactive substances on cancer and, on the other hand, for the cytoprotection of normal cells.[39]

3.3. Inspection of Stability of the Bound and Unbound Ligand Complex with PPRAδ. The molecular

https://doi.org/10.1021/acsomega.3c03705
ACS Omega 2023, 8, 33572−33579

docking study revealed a well-fit binding pattern by all of the compounds in the active site, but differences were observed in their modes of adopting interactions with active site residues of the PPRAδ protein. Furthermore, a molecular dynamics (MD) simulation study was conducted to illustrate the stability of all compound I complexes with the PPRAδ protein. Subsequently, it was observed that the potent compound (PPRAδ-C2) showed an energetically stabilized behavior in the binding site by adopting intermolecular interactions with active-site residues, such as hydrogen bonds and hydrophobic interactions, etc. In the present study, the binding mode for lauric acid, oleanolic acid, and bis(2-ethylhexyl) phthalate was investigated using molecular docking studies, further validating these docked complexes through MD simulation studies as shown in Figure 6A,B. The results indicate that the compounds

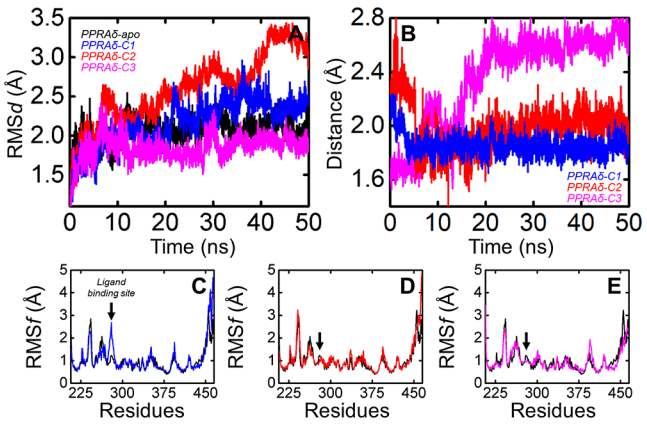

Figure 6. Molecular dynamics simulation in terms of RMSD and RMSF for PPARδ-apo and PPARδ-ligand complexes. The distance between the bound ligand and PPRAδ protein to explore the behavior of the compound in the active pocket concerning MD simulation time. (A) Superposed RMSD graph. (B) Superposed carbon alpha distance graph for APO and bound ligand complex with PPRAδ protein. Superpose RMSF graph of human PPARδ complexes with PPARδ-apo to show the fluctuation pattern throughout 50 ns molecular dynamics simulation time (C) for PPRAδ-apo and C1(Lauric acid), (D) for PPRAδ-apo and C2(oleanolic acid), and (E) for PPRAδ-apo and C3(bis(2-ethylhexyl) phthalate). The residue numbering is set according to the crystallographic structure.

(lauric acid, oleanolic acid, and bis(2-ethylhexyl) phthalate) exhibit significant binding affinities in adopting favorable interactions with active-site residues of human PPARδ protein.

MD simulation is one of the useful techniques to inspect the stability of docked protein−ligand complexes concerning the MD simulation time. MD simulations for each PPRAδ bound and unbound ligand complex were conducted via AMBER v14 to clearly illustrate the impact of the corresponding compound on the overall PPRAδ protein structure. The root mean square deviation (RMSD) was calculated based on the initial backbone coordinates of the protein−ligand complexes to evaluate the possible deviation in the structure during simulation and the RMSD of all PPRAδ bound. Unbound ligand complexes relative to the original structures show that a total simulation time of 50 ns is appropriate to reach equilibrium at the temperature 310 K. We observed that the RMSD of all PPRAδ complexes showed a similar deviation until 5 ns, but a dramatically changed behavior was observed, starting from 5 ns onward. This point deviation pins the point of the potential impact of the various compounds on the protein structure. Gradual increase was observed after the 10 ns simulation time. However, this deviation continued along the MD simulation time for complex PPRAδ-lauric acid and PPRAδ-bis(2-ethylhexyl) phthalate, but in the case of PPRAδ-oleanolic acid, it increased dramatically throughout the MD simulation time, as shown in Figure 6C,D. The sudden change in deviation might indicate the high potency of these compounds in complex with PPRAδ protein.

To understand the effect of individual amino acids on all of the complexes, including the PPRAδ bound and unbound ligand complex, we analyzed the root-mean-square fluctuations (RMSF). Consequently, from the RMSF graph, as shown in Figure 6E, it was observed that the RMSF values of most residues in all four systems showed similar fluctuations. Still, a dramatic swing occurred only in the ligand-binding site of the protein, where different compounds adopt various favorable interactions with active site residues.

Generally, from this data, we could assume that PPRAδ-oleanolic acid attained high fluctuation not only in the binding site but also in nearby residues, which further supports the high potency of these compounds and clearly illustrates the high profile of the ligand−protein interaction profile. While in the case of the other two complexes, for PPRAδ-lauric acid, a slight fluctuation was observed but comparatively less than the fluctuation pattern for PPRAδ-oleanolic acid. In the case of PPRAδ-bis(2-ethylhexyl) phthalate, a slightly weak change was found, which further indicates the inhibition pattern of this compound; no doubt, this compound attained inhibitory activity against the corresponding protein. More recently, carbon alpha distance analysis was conducted to explore the binding pattern concerning MD simulation time. Subsequently, it was observed that, in the case of PPRAδ-lauric acid and PPRAδ-bis(2-ethylhexyl) phthalate complexes, the Cα distance among the protein and ligand showed comparatively different behaviors, indicating that depending on the MD simulation time, the compounds attained various behaviors. While in the case of PPRAδ-oleanolic acid, a consistent behavior among the protein and oleanolic acid was observed, which further suggests that this compound sustains favorable interactions with the active site residues throughout the MD simulation time.

Additionally, the distance count profile was plotted to show the stability behavior of all of the ligand-bound complexes. This graph supports our distance analysis for the protein and ligand; the PPRAδ-oleanolic acid complex attained stable behaviors, but the other two compounds exhibited various behaviors with respect to time, which further indicates their less potency depending on the MD simulation time. These two compounds attained various pattern of interaction and in−out behavior, which is inappropriate for the high potency of the corresponding compounds.[40−44] The protein−ligand (PL) interactions for PPRAδ-lauric acid, PPRAδ-oleanolic acid, and PPRAδ-bis(2-ethylhexyl) phthalate profiles are depicted in Figure 7A−D.

4. CONCLUSIONS

HCC has the second highest mortality rate of all cancers, compelling scientists to research new therapeutics. Natural products are safe and account for half of the therapeutics available. The current research confirmed that the natural compounds lauric acid, oleanolic acid, and bis(2-ethylhexyl) phthalate inhibit proliferation, induce apoptosis, and induce cell death in HCC cells. The isolated compounds had cytotoxic effects. Thus, these compounds could be used as a source for

https://doi.org/10.1021/acsomega.3c03705
ACS Omega 2023, 8, 33572−33579

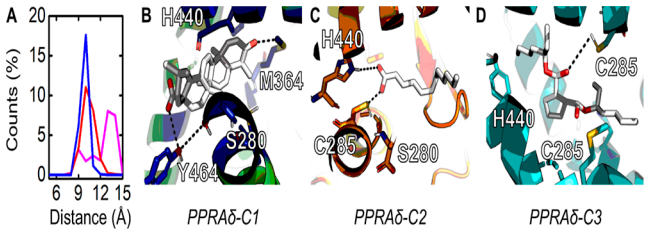

Figure 7. Post-MD simulation extracted structure, protein−ligand interaction, and the carbon alpha distance counts. (a) Carbon alpha distance counts demonstrated that PPRA*δ*-C2 was more stable regarding distance between the protein and C2 (oleanolic acid); this means that C2 showed smoothness in its behavior. In contrast, C1 (lauric acid) and C3 (bis(2-ethylhexyl) phthalate) were highly unstable and changed their conformation gradually. The protein−ligand interaction profiles for PPRA gamma with the ligand (B) for PPRA*δ*-C2, (C) for PPRA*δ*-C1, and (D) for PPRA*δ*-C3.

new lead structures in drug design to combat cancer. Furthermore, molecular docking and dynamics simulations revealed that these compounds had a high affinity for the target protein, as computationally predicted. As a result of further experimental validation, our findings may aid in the active treatment of HCC in the future. Furthermore, the strategy described herein is general and can be used against other carcinomas.

■ ASSOCIATED CONTENT

Data Availability Statement

The data sets generated and/or analyzed during the current study are available in the manuscript.

■ AUTHOR INFORMATION

Corresponding Authors

Bashir Ahmad − *Center of Biotechnology and Microbiology, University of Peshawar, Peshawar 25120, Pakistan*; Email: bashirdr2015@yahoo.com

Qurban Ali − *Department of Plant Breeding and Genetics, Faculty of Agricultural Sciences, University of the Punjab, Lahore 54590, Pakistan*; orcid.org/0000-0002-3160-4830; Email: saim1692@gmail.com

Authors

Said Hassan − *Institute of Biotechnology and Microbiology, Bacha Khan University Charsadda, Charsadda 24420, Pakistan*

Muhammad Waseem Khan − *Institute of Pharmaceutical Sciences, Khyber Medical University, Peshawar 25001, Pakistan*

Zafar Abbass Shah − *Department of Bioinformatics, Hazara University Mansehra, Mansehra 21300, Pakistan*

Amin Ullah − *Department of Health & Biological Sciences, Abasyn University, Peshawar 25120, Pakistan*

Sana Ullah − *Department of Zoology, Division of Science and Technology, University of Education, Lahore 54000, Pakistan*; orcid.org/0000-0002-9840-3988

Dilfaraz Khan − *Institute of Chemical Sciences, Gomal University, Dera Ismail Khan 29050, Pakistan*

Muhammad Rizwan − *Center for Biotechnology and Microbiology, Swat University, Swat 19130, Pakistan*

Ajaz Ahmad − *Department of Clinical Pharmacy, College of Pharmacy, King Saud University, Riyadh 11451, Saudi Arabia*

Prashant Kaushik − *Instituto de Conservación y Mejora de la Agrodiversidad Valenciana, Universitat Politècnica de València, Valencia 46022, Spain*

Semih Yilmaz − *Department of Agriculture Biotechnology, Division of Enzyme and Microbial Biotechnology, Erciyes University, Talas 38280, Turkey*

Complete contact information is available at: https://pubs.acs.org/10.1021/acsomega.3c03705

Author Contributions

Conceptualization, S.H. and B.A.; methodology, M.W.K.; software, S.U., A.U and M.R; validation, D.K., Z.A.S. and Q.A.; formal analysis, M.W.K.; investigation, M.R.; resources, Q.A., A.A and P.K.; data curation, S.H.; writing—original draft preparation, S.H and D.K.; writing—review and editing, D.K., Q.A., A.A., and B.A.; visualization, A.U., S.Y and S.H.; supervision, B.A.; project administration, B.A.; funding acquisition, A.A. All authors have read and agreed to the published version of the manuscript.

Funding

This research received no external funding.

Notes

The authors declare no competing financial interest.

Ethical approval and consent to participate: aerial parts of *M. buxifolia* (15 kg), a wild type fruiting plant grown in arid, semiarid climate conditions, collected from District Dir Lower, Khyber Pakhtunkhwa-Pakistan with voucher ID MBDDL20200103 and voucher specimens were deposited in a public herbarium of District Dir Lower. Dr. Jehandar Shah, the Taxonomist, Ex-Vice Chancellor Shaheed Benazir University Shiringal, Pakistan, authenticated the plant's samples. It has been confirmed that the experimental samples of plants, including the collection of plant material, complied with relevant institutional, national, and international guidelines and legislation with appropriate permissions from District authorities of Dir Lower Khyber Pakhtunkhwa-Pakistan for the collection of plant specimens.

■ ACKNOWLEDGMENTS

The authors would like to extend their sincere appreciation to the Researchers Supporting Project Number (RSP2023R350), King Saud University, Riyadh, Saudi Arabia.

■ REFERENCES

(1) Duke, J. A.; et al. *Natural Products from Plants*; CRC Press, 2016.

(2) Gonelimali, F. D.; Lin, J.; Miao, W.; Xuan, J.; Charles, F.; Chen, M.; Hatab, S. R. Antimicrobial properties and mechanism of action of some plant extracts against food pathogens and spoilage microorganisms. *Front. Microbiol.* **2018**, *9*, 9.

(3) Eisenberg, D. M.; Kessler, R. C.; Foster, C.; Norlock, F. E.; Calkins, D. R.; Delbanco, T. L. Unconventional medicine in the United States-prevalence, costs, and patterns of use. *N. Engl. J. Med.* **1993**, *328* (4), 246−252.

(4) Islam, M. S.; et al. Antitumor and phytotoxic activities of leaf methanol extract of Oldenlandia diffusa (willd.) roxb. *Global J. Pharmacol.* **2009**, *3* (2), 99−106.

(5) Amara, A. A.; El-Masry, M.; Bogdady, H. Plant crude extracts could be the solution: extracts showing in vivo antitumorigenic activity. *Pak. J. Pharm. Sci.* **2008**, *21* (2), 159.

(6) Abu-Dahab, R.; Afifi, F. Antiproliferative activity of selected medicinal plants of Jordan against a breast adenocarcinoma cell line (MCF7). *Sci. Pharm.* **2007**, *75* (3), 121−136.

(7) Mutha, R. E.; Shimpi, R. D.; Jadhav, R. B. Study of preliminary anticancer potential of some hemiparasite plants. *Int. J. Pharm. Res. Dev.* **2010**, *2*, 1.
(8) Gonzales, G. F.; Valerio, L. G. Medicinal plants from Peru: a review of plants as potential agents against cancer. *Anti Cancer Agents Med. Chem.* **2006**, *6* (5), 429−444.
(9) Cragg, G. M.; Grothaus, P. G.; Newman, D. J. Impact of natural products on developing new anti-cancer agents. *Chem. Rev.* **2009**, *109* (7), 3012−3043.
(10) Li, Y.; Martin, R. C. Herbal medicine and hepatocellular carcinoma: applications and challenges. *Evid. base Compl. Alternative Med.* **2011**, *2011*, 2011−2014.
(11) Choo, S. P.; Tan, W. L.; Goh, B. K. P.; Tai, W. M.; Zhu, A. X. Comparison of hepatocellular carcinoma in E astern versus W estern populations. *Cancer* **2016**, *122* (22), 3430−3446.
(12) Albarrak, J.; Al-Shamsi, H. Current Status of Management of Hepatocellular Carcinoma in The Gulf Region: Challenges and Recommendations. *Cancers* **2023**, *15* (7), 2001.
(13) Hassan, S.; Ahmad, B.; Khan, S. U.; Linfang, H.; Anjum, S. I.; Ansari, M. J.; Rahman, K.; Ahmad, I.; Khan, W. U.; Qamar, R.; et al. In vivo pharmacological investigation of Monotheca buxifolia and Bosea amherstiana using animal models. *Saudi J. Biol. Sci.* **2019**, *26*, 1602−1606.
(14) Nasir, E.; Ali, S.; Stewart, R. R. *Flora of West Pakistan*; Pakistan Agricultural Research Council, 1972.
(15) Hassan, S.; Ahmad, B.; Khan, S. U.; Linfang, H.; Anjum, S. I.; Ansari, M. J.; Rahman, K.; Ahmad, I.; Khan, W. U.; Qamar, R.; et al. In vivo pharmacological investigation of Monotheca buxifolia and Bosea amherstiana using animal models. *Saudi J. Biol. Sci.* **2019**, *26* (7), 1602−1606.
(16) Hassan, S.; et al. Protective role of Monotheca buxifolia and Bosea amherstiana against H 2 O 2-induced DNA damage in human lymphocytes and its effect on oxidative enzymes. *Pak. J. Pharm. Sci.* **2019**, *32*(2), 601−606.
(17) Chabán, M. F.; Karagianni, C.; Joray, M. B.; Toumpa, D.; Sola, C.; Crespo, M. I.; Palacios, S. M.; Athanassopoulos, C. M.; Carpinella, M. C. Antibacterial effects of extracts obtained from plants of Argentina: Bioguided isolation of compounds from the anti-infectious medicinal plant Lepechinia meyenii. *J. Ethnopharmacol.* **2019**, *239*, 111930.
(18) Gayathri, L.; Dhivya, R.; Dhanasekaran, D.; Periasamy, V. S.; Alshatwi, A. A.; Akbarsha, M. A. Hepatotoxic effect of ochratoxin A and citrinin, alone and in combination, and protective effect of vitamin E: In vitro study in HepG2 cell. *Food Chem. Toxicol.* **2015**, *83*, 151−163.
(19) Li, Z.; Lan, Y.; Miao, J.; Chen, X.; Chen, B.; Liu, G.; Wu, X.; Zhu, X.; Cao, Y. Phytochemicals, antioxidant capacity and cytoprotective effects of jackfruit (Artocarpus heterophyllus Lam.) axis extracts on HepG2 cells. *Food Biosci.* **2021**, *41*, 100933.
(20) Farshori, N. N.; Al-Sheddi, E. S.; Al-Oqail, M. M.; Musarrat, J.; Al-Khedhairy, A. A.; Siddiqui, M. A. Cytotoxicity Assessments of Portulaca oleraceaand Petroselinum sativum Seed Extracts on Human Hepatocellular Carcinoma Cells (HepG2). *Asian Pac. J. Cancer Prev.* **2014**, *15* (16), 6633−6638.
(21) Cheng, Y.; Zhao, P.; Wu, S.; Yang, T.; Chen, Y.; Zhang, X.; He, C.; Zheng, C.; Li, K.; Ma, X.; et al. Cisplatin and curcumin co-loaded nano-liposomes for the treatment of hepatocellular carcinoma. *Int. J. Pharm.* **2018**, *545* (1−2), 261−273.
(22) Wu, H.; Zhong, Q.; Zhong, R.; Huang, H.; Xia, Z.; Ke, Z.; Zhang, Z.; Song, J.; Jia, X. Preparation and antitumor evaluation of self-assembling oleanolic acid-loaded Pluronic P105/D-α-tocopheryl polyethylene glycol succinate mixed micelles for non-small-cell lung cancer treatment. *Int. J. Nanomed.* **2016**, *11*, 6337−6352.
(23) Chemical Computing Group Inc. *Molecular Operating Environment (MOE)*; Chemical Computing Group Inc.: 1010 Sherbooke St. West, Suite# 910, Montreal, 2016.
(24) Qureshi, N. A.; Bakhtiar, S. M.; Faheem, M.; Shah, M.; Bari, A.; Mahmood, H. M.; Sohaib, M.; Mothana, R. A.; Ullah, R.; Jamal, S. B. Genome-based drug target identification in human pathogen Streptococcus gallolyticus. *Front. Genet.* **2021**, *12*, 564056.
(25) Cronet, P.; Petersen, J. F.; Folmer, R.; Blomberg, N.; Sjöblom, K.; Karlsson, U.; Lindstedt, E. L.; Bamberg, K. Structure of the PPARα and-γ ligand binding domain in complex with AZ 242; ligand selectivity and agonist activation in the PPAR family. *Structure* **2001**, *9* (8), 699−706.
(26) Faheem, M.; Jamal, S. B. Identification of Zika virus NS5 novel inhibitors through virtual screening and docking studies. *Life Sci.* **2020**, *1* (1), 5.
(27) Darden, T.; York, D.; Pedersen, L. Particle mesh Ewald: An N·log (N) method for Ewald sums in large systems. *J. Chem. Phys.* **1993**, *98* (12), 10089−10092.
(28) Wadood, A.; Riaz, M.; Jamal, S. B.; Shah, M. Interactions of ketoamide inhibitors on HCV NS3/4A protease target: molecular docking studies. *Mol. Biol. Rep.* **2014**, *41*, 337−345.
(29) Aytenfisu, A. H.; Spasic, A.; Grossfield, A.; Stern, H. A.; Mathews, D. H. Revised RNA dihedral parameters for the Amber force field improve RNA molecular dynamics. *J. Chem. Theory Comput.* **2017**, *13* (2), 900−915.
(30) Berendsen, H. J.; van der Spoel, D.; van Drunen, R. GROMACS: a message-passing parallel molecular dynamics implementation. *Comput. Phys. Commun.* **1995**, *91* (1−3), 43−56.
(31) Al-Lihaibi, S. S.; Alarif, W. M.; Abdel-Lateff, A.; Ayyad, S. E. N.; Abdel-Naim, A. B.; El-Senduny, F. F.; Badria, F. A. Three new cembranoid-type diterpenes from Red Sea soft coral Sarcophyton glaucum: Isolation and antiproliferative activity against HepG2 cells. *Eur. J. Med. Chem.* **2014**, *81*, 314−322.
(32) Elshafie, H. S.; Armentano, M.; Carmosino, M.; Bufo, S.; De Feo, V.; Camele, I. Cytotoxic activity of Origanum vulgare L. on hepatocellular carcinoma cell line HepG2 and evaluation of its biological activity. *Molecules* **2017**, *22* (9), 1435.
(33) Zhivotosky, B.; Orrenius, S. Assessment of apoptosis and necrosis by DNA fragmentation and morphological criteria. *Curr. Protoc. Cell Biol.* **2001**, *12* (1), 18.3.1−18.3.23.
(34) Matassov, D.; et al. Measurement of apoptosis by DNA fragmentation. *Apoptosis Methods and Protocols*; Springer, 2004; pp 1−17.
(35) Errami, Y.; Naura, A. S.; Kim, H.; Ju, J.; Suzuki, Y.; El-Bahrawy, A. H.; Ghonim, M. A.; Hemeida, R. A.; Mansy, M. S.; Zhang, J.; et al. Apoptotic DNA fragmentation may be a cooperative activity between caspase-activated deoxyribonuclease and the poly (ADP-ribose) polymerase-regulated DNAS1L3, an endoplasmic reticulum-localized endonuclease that translocates to the nucleus during apoptosis. *J. Biol. Chem.* **2013**, *288* (5), 3460−3468.
(36) Zhang, M.; et al. BAPTA blocks DNA fragmentation and chromatin condensation downstream of caspase-3 and DFF activation in HT-induced apoptosis in HL-60 cells. *Apoptosis* **2001**, *6* (4), 291−297.
(37) Liu, J.; Ma, L.; Chen, X.; Wang, J.; Yu, T.; Gong, Y.; Ma, A.; Zheng, L.; Liang, H. ERK inhibition sensitizes cancer cells to oleanolic acid-induced apoptosis through ERK/Nrf2/ROS pathway. *Tumor Biol.* **2016**, *37* (6), 8181−8187.
(38) Akl, M. R.; Elsayed, H. E.; Ebrahim, H. Y.; Haggag, E. G.; Kamal, A. M.; El Sayed, K. A. 3-O-[N-(p-fluorobenzenesulfonyl)-carbamoyl]-oleanolic acid, a semisynthetic analog of oleanolic acid, induces apoptosis in breast cancer cells. *Eur. J. Pharmacol.* **2014**, *740*, 209−217.
(39) Liu, J.; Wu, N.; Ma, L. N.; Zhong, J. T.; Liu, G.; Zheng, L. H.; Lin, X. K. p38 MAPK signaling mediates mitochondrial apoptosis in cancer cells induced by oleanolic acid. *Asian Pac. J. Cancer Prev.* **2014**, *15* (11), 4519−4525.
(40) Khan, M. T.; Rehaman, A. U.; Junaid, M.; Malik, S. I.; Wei, D. Q. Insight into novel clinical mutants of RpsA-S324F, E325K, and G341R of Mycobacterium tuberculosis associated with pyrazinamide resistance. *Comput. Struct. Biotechnol. J.* **2018**, *16*, 379−387.
(41) Qin, F.; Chen, Y.; Wu, M.; Li, Y.; Zhang, J.; Chen, H. F. Induced fit or conformational selection for RNA/U1A folding. *RNA* **2010**, *16* (5), 1053−1061.

https://doi.org/10.1021/acsomega.3c03705
ACS Omega 2023, 8, 33572−33579

(42) Miller, B. R.; McGee, T. D.; Swails, J. M.; Homeyer, N.; Gohlke, H.; Roitberg, A. E. MMPBSA. py: an efficient program for end-state free energy calculations. *J. Chem. Theory Comput.* **2012**, *8* (9), 3314−3321.
(43) Chen, H.-F. Mechanism of coupled folding and binding in the siRNA-PAZ complex. *J. Chem. Theory Comput.* **2008**, *4* (8), 1360−1368.
(44) Wang, J.; Cai, Q.; Xiang, Y.; Luo, R. Reducing grid dependence in finite-difference Poisson-Boltzmann calculations. *J. Chem. Theory Comput.* **2012**, *8* (8), 2741−2751.

https://doi.org/10.1021/acsomega.3c03705
ACS Omega 2023, 8, 33572−33579